Open Access Full Text Article

ORIGINAL RESEARCH

Simple and effective label-free electrochemical immunoassay for carbohydrate antigen 19-9 based on polythionine-Au composites as enhanced sensing signals for detecting different clinical samples

Zhengjun Huang[1,2]
Zhouqian Jiang[1,2]
Chengfei Zhao[1,2]
Wendi Han[3]
Liqing Lin[1,2]
Ailin Liu[1,2]
Shaohuang Weng[1,2]
Xinhua Lin[1,2]

[1]Department of Pharmaceutical Analysis, School of Pharmacy, Fujian Medical University, [2]Higher Educational Key Laboratory for Nano Biomedical Technology of Fujian Province, [3]Department of Pharmacy, The First Affiliated Hospital of Fujian Medical University, Fuzhou, People's Republic of China

Correspondence: Liqing Lin;
Shaohuang Weng
Department of Pharmaceutical Analysis, School of Pharmacy, Fujian Medical University, 1 North Xuefu Road, Fuzhou, Fujian 350122, People's Republic of China
Tel/fax +86 591 2286 2016
Email fjmu_lin@126.com;
shweng@fjmu.edu.cn

Abstract: Carbohydrate antigen 19-9 (CA19-9) is an important biomarker for the early diagnosis and clinical monitoring of pancreatic cancer. Reliable, simple, and accurate methods for the detection of CA19-9 are still urgently needed. In this study, polythionine-Au composites (AuNPs@PThi) were designed and prepared through one-pot reaction using $HAuCl_4$ as the co-oxidant and raw material in thionine solution containing $FeCl_3$ as the oxidant. AuNPs@PThi-immobilized glassy carbon electrode was used as a sensitive redox probe for electrochemical interface. AuNPs@PThi not only favored the amplification of electrochemical signals but also facilitated excellent environmental friendliness for bioassay. Maximizing the electrochemical properties of AuNPs@PThi, an effective label-free electrochemical immunoassay for the ultrasensitive and reliable detection of CA19-9 was developed. Under optimal conditions, the linear range of the proposed immunosensor was estimated to range from 6.5 to 520 U/mL, with a detection limit of 0.26 U/mL at a signal-to-noise ratio of 3. The prepared immunosensor for CA19-9 detection showed high sensitivity, stability, and reproducibility. Furthermore, the fabricated immunosensor based on AuNPs@PThi can effectively detect and distinguish clinical serum samples of pancreatic cancer and normal control with accuracy and convenience.

Keywords: polythionine-Au composites, label-free electrochemical immunoassay, carbohydrate antigen 19-9, clinical sample, signal amplification

Introduction

Pancreatic cancer is the ninth most common malignant tumor in China.[1] The 5-year survival rate of pancreatic cancer patients is <5% because of the high degree of malignancy of the disease.[2] Pancreatic cancer shows the worst prognosis among malignant tumors. This disease usually shows a short time window before clinical diagnosis.[3,4] Furthermore, pancreatic cancer patients are expected to be cured through early diagnosis and surgery.[5] Therefore, early diagnosis is important in the treatment efficacy and quality of life of pancreatic cancer patients.

Tumor markers are molecules found in blood, tissue, and body fluids, and their measurement or identification is useful in patient diagnosis or clinical management.[6] During tumorigenesis, altered levels of tumor markers in patients are associated with a certain tumor. Carbohydrate antigen 19-9 (CA19-9) is a glycoprotein highly associated with malignant tumors and commonly used as a clinical marker for the

diagnosis of pancreatic cancer, colorectal cancer, and gastric carcinoma, particularly pancreatic carcinoma.[7,8] The CA19-9 levels of normal adults are significantly lower than 37 U/mL.[9] However, a slight elevation of CA19-9 level in blood is closely related to pancreatic cancer incidence and development.[10] A sensitive and accurate determination of CA19-9 is crucial for the early clinical diagnosis of pancreatic cancer.

Traditional immunoassay methods for tumor markers include fluorescence,[11,12] spectroscopy,[13,14] chemiluminescence,[15,16] radioimmunoassay,[17,18] electrophoresis,[19] polymerase chain reaction (PCR), and enzyme-linked immunosorbent assay (ELISA).[20–22] Current methods can obtain accurate and reliable detection results but usually require expensive instruments and complex operating procedures. The development of a new, facile, and cost-effective technology with improved sensitivity to detect tumor markers is urgently needed to facilitate the early diagnosis and treatment of tumors.[23–25] Electrochemical immunosensors, which are a novel type of biosensors that combine electrochemical sensing technology and immunoassay technology, feature high sensitivity and specificity; thus, these biosensors can be applied to the analytical investigation of monitoring immunogenicity and its response.[26,27] Label-free electrochemical immunosensors, which feature easy control, simple apparatus, and low price, can be explored to detect different biological molecules.[28,29]

The efficient immobilization of antibodies and the generation with amplified signals are the key steps in constructing label-free electrochemical immunosensors.[30,31] The emergence of new nanomaterials has opened a new approach to develop such sensors. In recent years, several nanocomposites or their redox products have been gradually used to design and build a novel biosensing interface because of their good electrochemical activity and strong adsorption ability.[32–36] In the development of new biosensing interface, label-free style electrochemical sensor, with the introduction of special redox mediator for specific target biomarkers, is attractive. The electron mediator thionine can be used to construct label-free electrochemical immunosensors because of its favorable electron transfer capability; however the stability of the electrode remains to be improved. Compared with its monomer, polythionine features larger specific surface area, higher reaction activity, and long-term stability.[37,38] Regulation of polythionine can improve the ability and application performance in electrochemical biosensors.[39–42] Anionic surfactant-doped polythionine with sensitive response was recently prepared and used for the fabrication of label-free electrochemical immunosensor.[39] The previous work reported that polythionine and gold nanocomposites can be effectively synthesized and applied to detect biomarkers with high isoelectric point.[40] Although reported works illustrated the fact that specific electrochemical biosensors for some targets based on polythionine or its composites can be obtained, the construction of facile label-free electrochemical sensing interface for large-scale analysis of biomarkers for variable clinical samples is still not available.

The present study aims to explore a label-free electrochemical immunosensor based on polythionine-Au composites (AuNPs@PThi) and Au nanoparticles for CA19-9 detection. The abovementioned immunosensor not only favors signal amplification but also improves stability, selectivity, sensitivity, and reproducibility. It provides a new path for the scientific basis of clinical applications based on AuNPs@PThi. The resulting label-free electrochemical immunosensor could be used to accurately detect CA19-9 sensitively and facilely in a large number of clinical samples. Thus, the method established in this work was used to detect and differentiate CA19-9 concentration in pancreatic cancer patients and healthy controls.

Materials and methods
Chemicals and materials

CA19-9 antibody was obtained from Abcam Co., Ltd., Cambridge, UK. CA19-9 antigen was obtained from Siemens Co., Ltd., Berlin, Germany. N,N-Dimethylformamide (DMF), chloroauric acid solution ($HAuCl_4 \cdot 4H_2O$), $C_6H_5NaO_7 \cdot 2H_2O$, $K_4[Fe(CN)_6] \cdot 2H_2O$, and $K_3[Fe(CN)_6]$ were purchased from Sinopharm Chemical Reagent Co., Ltd. (Shanghai, China). Thionine ($C_{14}H_{13}N_3O_2S$) and bovine serum albumin (BSA) were obtained from Sigma-Aldrich Co. LLC, St Louis, MO, USA. All chemicals were of analytical grade, and all stock solutions were prepared using deionized or autoclaved water.

Apparatus

The electrochemical measurement was performed with a CHI 660C electrochemical analytical system (CH Instrument, Inc., Shanghai, China) connected to a personal computer. All electrochemical measurements were carried out with a conventional three-electrode system composed of a glassy carbon electrode (GCE, 3 mm in diameter), a platinum wire counter electrode, and an Ag/AgCl (saturated KCl solution) reference electrode. Electrochemical impedance spectroscopy (EIS) were performed on an Autolab PGSTAT302F system (Eco Chemie Co., Ltd., Utrecht, the Netherlands). Transmission electron microscopy (TEM) was operated on a JEM-1400 system (JEOL Co., Ltd., Tokyo, Japan) with an accelerating

applied potential of 100 kV. Atomic force microscopy (AFM) was performed on a NanoScope VIII system (Bruker Co., Ltd., Karlsruhe, Germany). All the experiments were carried out at ambient temperature.

Synthesis of AuNPs

AuNPs were prepared via reduction of $HAuCl_4$ by sodium citrate, according to an established method.[43] In short, 4 mL of 1% sodium citrate solution was added into 250 mL of boiled 0.01% $HAuCl_4$ solution rapidly, followed by keeping the mixture solution boiling for another 10 min under stirring. As-formed AuNPs solution was stored at 4°C for further use.

Preparation of AuNPs@PThi

In a 250 mL round bottom flask, with the temperature controlled at 50°C, 0.08 g thionine, 1 mL 1% $HAuCl_4$, and 1 mL 30% H_2O_2 were successively added into the 50 mL 6 mM $FeCl_3$ solution under vigorous stirring for 24 h. Afterward, the obtained black liquor was centrifuged, and then the precipitate was successively washed with 0.1 mol/L HCl and deionized water three times to remove impurities, by-product, and excess ions. Then, the black powder was dried in vacuum at 40°C for 8 h to get the final product. Pristine PThi was prepared through the same procedure as AuNPs@PThi, just without the addition of $HAuCl_4$.

Synthesis of AuNPs/AuNPs@PThi/GCE

The AuNPs/AuNPs@PThi/GCE was prepared by adsorption of citrate-stabilized AuNPs onto the GCE using AuNPs@ PThi as a cross-linking agent. In a typical synthesis, 4 µL of 0.5 mg/mL AuNPs@PThi dispersed in DMF solution was dropped on the surface of pretreated GCE and left to dry at room temperature, followed by adding 5 µL of AuNPs collosol and leaving at room temperature for 12 h to form AuNPs/AuNPs@PThi/GCE. As-prepared electrode was stored at 4°C for further use.

Fabrication of the immunosensor

The immunosensor was fabricated by a simple casting method. First, 10 µL of 100 µg/mL anti-CA19-9 was dropped on the surface of the prepared AuNPs/AuNPs@PThi/GCE and then incubated for 60 min to form the anti-CA19-9/AuNPs/AuNPs@PThi/GCE after washing with phosphate buffer and drying in a stream of nitrogen. Following that, the above GCE was incubated in 0.1% BSA solution for 30 min to eliminate nonspecific binding. Subsequently, the BSA/anti-CA19-9/AuNPs/AuNPs@PThi/GCE detection electrode was succeeded after washing with phosphate buffer and drying in a stream of nitrogen. Finally, the electrode was incubated with a series of concentrations of CA19-9 solution for 60 min, and the electrochemical signal before and after the binding of CA19-9 was tested and compared. Figure 1 displays the fabricated procedure and the measurement protocol of the electrochemical immunosensor.

Results and discussion
Characterization of AuNPs@PThi

The morphology and inherent electrochemical property of AuNPs@PThi may affect the testing performance of the fabricating sensor. The characterization of AuNPs@PThi was conducted first. Figure 2A shows the transmission electron
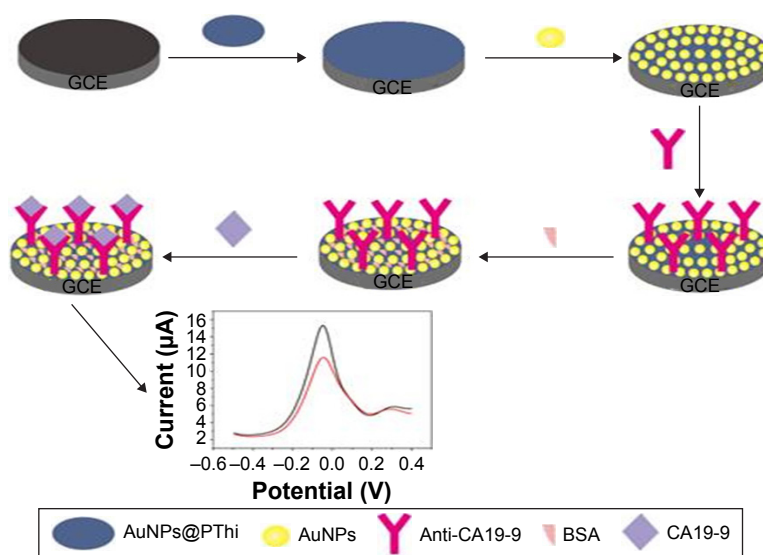

Figure 1 Schematic illustration of the label-free electrochemical immunosensor for CA19-9 detection.
Abbreviations: CA19-9, carbohydrate antigen 19-9; AuNPs@PThi, polythionine-Au composites; BSA, bovine serum albumin; GCE, glassy carbon electrode.
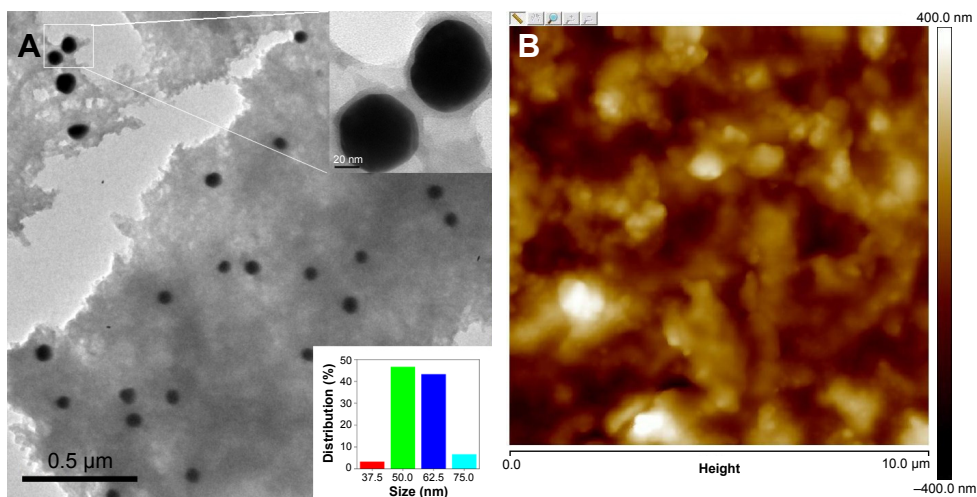
Figure 2 Transmission electron microscopic (**A**) and atomic force microscopic (**B**) images of AuNPs@PThi.
Note: The inset of (**A**) illustrates the amplification (upper) and distribution (bottom) of AuNPs in AuNPs@PThi.
Abbreviation: AuNPs@PThi, polythionine-Au composites.

microscopic image of the as-formed AuNPs@PThi. A thin and uniform PThi layer was coated on the surface of 50 nm subglobular AuNPs. The composites were well separated from each other. The typical atomic force microscopic image in Figure 2B shows that AuNPs@PThi-modified GCE exhibited a homogeneous, orderly, and sheet form. Hence, AuNPs@PThi can successfully and effectively form and modify on the surface of GCE.

The electrochemical property of the prepared AuNPs@PThi was investigated and compared to confirm whether the AuNPs@PThi owned the superiority than the pure polythionine. Thus, the same contents of PThi and AuNPs@PThi were used to prepare the modified electrode, and the cyclic voltammetry (CV) performance was tested. As shown in Figure 3, PThi and AuNPs@PThi both exhibited quasireversible redox behavior with ΔEp values of 109 and 107 mV, respectively. In addition, the reduction and oxidation peak currents of AuNPs@PThi increased compared with the same content of simple PThi. The electroactive behavior of AuNPs@PThi was superior to that of PThi because of the introduction of AuNPs. Furthermore, AuNPs@PThi effectively improved the electrochemical response, illustrating the possible improvement of sensing performance.

Characterization of immunosensor fabrication

According to the excellent electrochemical property of AuNPs@PThi, differential pulse voltammetry (DPV) was used to investigate the varied signals and to monitor the fabrication of the proposed immunosensor based on the

immobilized AuNPs@PThi, as shown in Figure 4. Compared with no peak on GCE (curve a), curve b shows an apparent anodic peak of AuNPs@PThi at approximately 0.01 V because of the internal response of the prepared AuNPs@PThi. The electrode electrochemical response indicated the sensitive response of AuNPs@PThi/GCE. After AuNP assembly, AuNPs/AuNPs@PThi/GCE exhibited a strengthened current (curve c), implying that the transfer rate was improved due to the formation of an AuNP layer with enhanced current transfer. For anti-CA19-9 immobilization, anti-CA19-9/AuNPs/AuNPs@PThi/GCE exhibited further enhanced current response (curve d). The improved current was markedly different from the inhibited behavior of antibody immobilization of the immunosensor with AuNPs@PThi as the signal.[37,44,45] When the pH of the
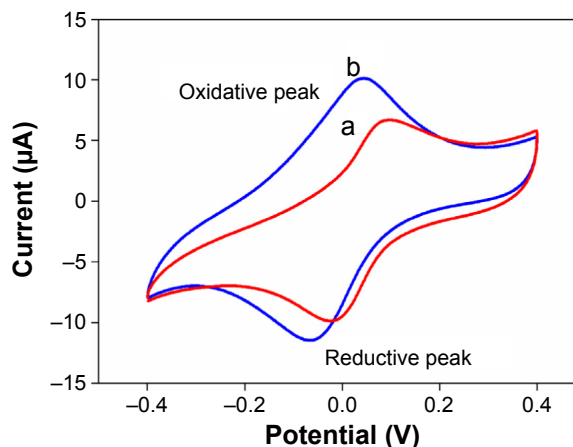

Figure 3 CV of PThi (a) and AuNPs@PThi (b) in 0.1 mol/L PBS with pH 3.5.
Abbreviations: CV, cyclic voltammetry; AuNPs@PThi, polythionine-Au composites; PBS, phosphate-buffered saline.
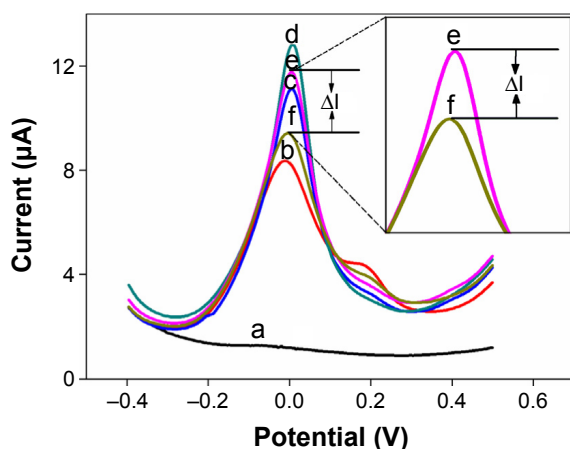
Figure 4 DPV responses of GCE (a), AuNPs@PThi/GCE (b), AuNPs/AuNPs@PThi/GCE (c), anti-CA19-9/AuNPs/AuNPs@PThi/GCE (d), BSA/anti-CA19-9/AuNPs/AuNPs@PThi/GCE (e), and CA19-9/BSA/anti-CA19-9/AuNPs/AuNPs@PThi/GCE (f) in PBS (pH 3.5) for the different steps of the label-free immunosensor.
Note: The inset shows the amplified section of varied current (ΔI) between curve e and curve f due to the formation of immunoreactions exposed to CA19-9.
Abbreviations: DPV, differential pulse voltammetry; GCE, glassy carbon electrode; AuNPs@PThi, polythionine-Au composites; CA19-9, carbohydrate antigen 19-9; BSA, bovine serum albumin; PBS, phosphate-buffered saline.

detecting solution was 3.5, the immobilized anti-CA19-9 may adjust the surface charge of the electrode.[40] The modulated surface structure and surface charge promoted the current transfer between the electrode and the electrolyte in a total sensing loop and improved the response current.[46] Subsequently, when the electrode was modified with BSA to eliminate nonspecific binding, the peak current decreased because of the formation of an electron-blocking layer. Finally, the current response obviously decreased compared with curve e because of the insulating CA19-9 protein layers on the electrode that hinder the electron transfer. Thus, using AuNPs@PThi as the signal indicator and AuNPs as the antibody carrier, we can calculate CA19-9 concentration from the current before and after the formation of the immunocomplex (ΔI) with added CA19-9.

Correspondingly, electrochemical impedance spectra were used to investigate the surface changes in the modification process of the immunosensor. As shown in Figure 5, a semicircle portion at high frequencies and a linear portion at low frequencies were obtained at different electrode assembly steps. Using $[Fe(CN)_6]^{3-/4-}$ as the electrochemical probe, various electron-transfer resistances (R_{et}) of different electrodes exhibited successful fabrication of the immunosensor. The R_{et} of AuNPs@PThi/GCE (4,375 Ω, curve b) was larger than that of the bare GCE (500 Ω, curve a), suggesting the successful assembly of AuNPs@PThi.

With the assembly of AuNPs, R_{et} decreased to 1,675 Ω (curve c) compared with that of AuNPs@PThi/GCE, illustrating the accelerated electron transfer effect because of the high
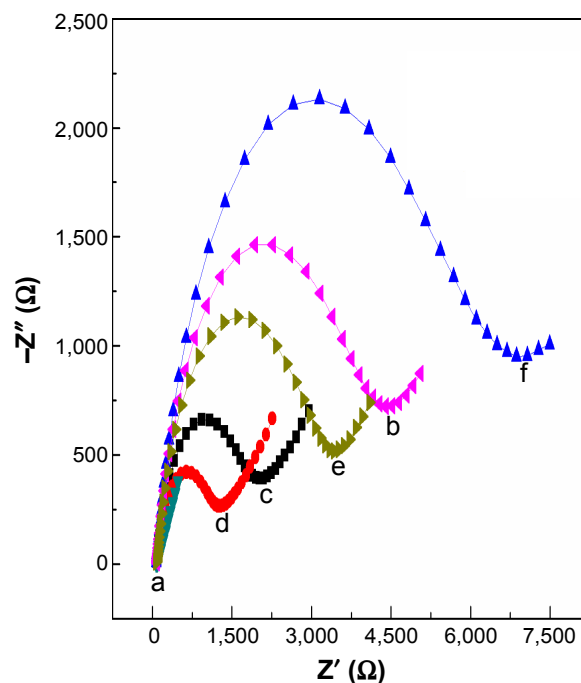

Figure 5 EIS of GCE (a), AuNPs@PThi/GCE (b), AuNPs/AuNPs@PThi/GCE (c), anti-CA19-9/AuNPs/AuNPs@PThi/GCE (d), BSA/anti-CA19-9/AuNPs/AuNPs@PThi/GCE (e), and CA19-9/BSA/anti-CA19-9/AuNPs/AuNPs@PThi/GCE (f) in 10 mmol/L $[Fe(CN)_6]^{3-}/[Fe(CN)_6]^{4-}$ and 0.1 mol/L KCl from 0.1 Hz to 100 kHz.
Abbreviations: GCE, glassy carbon electrode; AuNPs@PThi, polythionine-Au composites; CA19-9, carbohydrate antigen 19-9; BSA, bovine serum albumin; EIS, electrochemical impedance spectroscopy.

conductivity of AuNPs. When the anti-CA19-9 immobilized on the surface of AuNPs/AuNPs@PThi/GCE, the value of R_{et} further decreased (curve d), which agreed with the results of DPV. After the capture of BSA and CA19-9, the values of R_{et} increased to 3,500 Ω (curve e) and then to 6,875 Ω (curve f). This result suggests that the formation of the immunocomplex layer hindered the electron transfer. Therefore, the results of DPV and EIS of the different assembly steps of the proposed immunosensor confirmed the feasibility of the sensing of CA19-9 through such a method.

Optimization of experimental conditions
The signal source of the immunosensor was the introduction of AuNPs@PThi. Thus, the origin of the electrochemical response of the AuNPs@PThi-modified GCE is important for the sensing performance of the immunoassay. The concentration of AuNPs@PThi for the modified electrode was initially investigated, as shown in Figure 6A. AuNPs@PThi at concentrations between 0.05 and 5 mg/mL significantly increased the reduction peak current but exerted no significant influence at greater concentrations. For convenience, 5 mg/mL AuNPs@PThi was used for electrode modifications. The quantitative basis of CA19-9 was ΔI due to the introduction of CA19-9 to the antibody-modified electrode. Thus, several
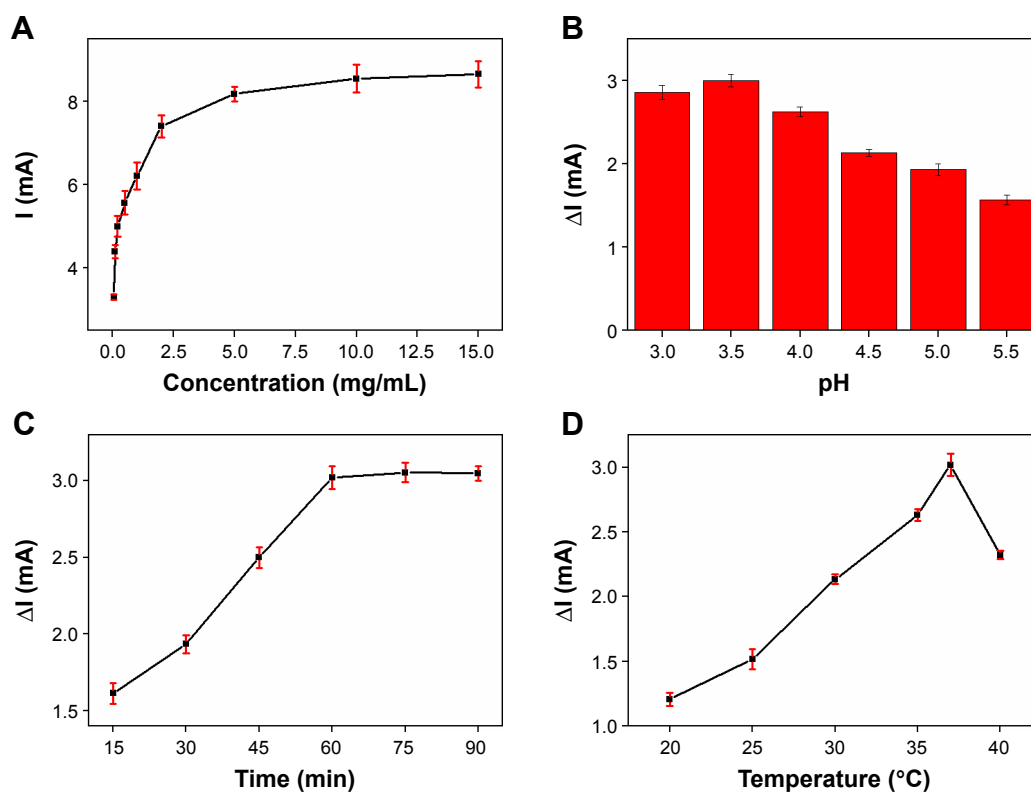
Figure 6 Effects of the original response (I) of the concentration of AuNPs@PThi (**A**), and effects of pH (**B**), incubation time (**C**), and incubation temperature (**D**) of immunoreaction on the ΔI of the recognition 100 U/mL CA19-9 using the proposed immunosensor.
Note: Error bars represent the SDs from three independent detections.
Abbreviations: AuNPs@PThi, polythionine-Au composites; CA19-9, carbohydrate antigen 19-9; SD, standard deviation.

factors, including the pH of the sensing solution, reaction temperature, and reaction time, were optimized. Solution pH significantly affected the electrochemical behavior of the immunosensor because the acidity of the solution may influence the activity of the immobilized protein and the response of AuNPs@PThi. To optimize the pH, a series of phosphate-buffered saline (PBS) buffer with pH 3.0–5.5 was prepared and ΔI was compared through DPV. Figure 6B shows that the current response (ΔI) increased and then decreased in the pH range of 3.0 to 5.5 with a maximum value at pH 3.5. Therefore, pH 3.5 of the detection solution was chosen as the optimal solution to obtain high sensitivity. Incubation time is another important parameter in the construction of the immunosensor. The effect of incubation time was investigated within the time range of 15–90 min with 10 U/L CA19-9. Figure 6C shows that the current response rapidly increased within 30 and 60 min and then tended to level off due to the saturated formation of an antigen–antibody complex. Therefore, the optimal incubation time was set at 60 min. We also investigated the effect of temperature on the reaction. Figure 6D shows the effect of different temperatures (20°C–40°C) on the current responses. The peak current increased with increasing temperature, reached the maximum

value at 37°C, and then decreased at temperatures over 37°C. This result may be attributed to the irreversible behavior (protein denaturation) involved in the process, which is caused by high temperatures. Thus, the optimal incubation temperature to achieve immunoreaction was 37°C.

Detection performance of the electrochemical immunosensor

Under the optimal conditions, different concentrations of CA19-9 in the incubation solution were detected by DPV. Figure 7 shows the DPV curves of the constructed BSA/anti-CA19-9/AuNPs/AuNPs@PThi/GCE after immunoreaction with different concentrations of CA19-9. The peak currents of AuNPs@PThi proportionately decreased with increasing concentrations of CA19-9. Typically, CA19-9 was attached to the electrode surface through immunoreaction with anti-CA19-9, which was previously immobilized on the immunosensor. The insulating CA19-9 protein layer acting as a nonconductor obstructed the electron transfer between the electrolyte and the electrode surface. Therefore, the DPV peak currents decreased proportionally with increasing CA19-9 concentration, which can be utilized as a quantitative measurement of CA19-9 concentration.[47]
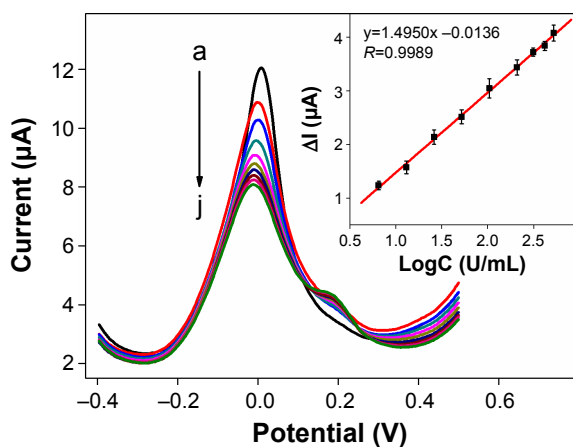
Figure 7 DPV responses to different concentrations of CA19-9 (from a to j: 0, 6.5, 13, 26, 52, 104, 208, 312, 416, and 520 U/mL) in the PBS.
Notes: The inset shows the linear relationship between ΔI and the logarithm of CA19-9 concentrations. The error bars represent the SDs from three independent detections.
Abbreviations: DPV, differential pulse voltammetry; CA19-9, carbohydrate antigen 19-9; PBS, phosphate-buffered saline; SD, standard deviation.

Figure 8 Specificity of the electrochemical immunosensor toward 5 ng/mL common proteins and digestive enzymes (5 U/mL for CA125 and CA19-9).
Note: Error bars represent the SDs from three independent detections.
Abbreviations: CA19-9, carbohydrate antigen 19-9; BSA, bovine serum albumin; SD, standard deviation; AFP, alpha fetoprotein; CEA, carcinoembryonic antigen.

As presented in Figure 7, decreased currents (ΔI) showed a linear relation with the logarithm of CA19-9 concentrations in the range of 6.5–520 U/mL. The linear equation was ΔI (μA) =−0.0136+1.4950 LogC (U/mL) with R=0.9989, and the limit of detection was calculated to be 0.26 U/mL at a signal-to-noise ratio of 3.

Several common interfering proteins, including digestive enzymes and tumor markers, were tested to evaluate the specificity of the proposed immunosensor. The ΔI values of the immunosensor toward interfering proteins were obtained under the same experimental condition for CA19-9, as shown in Figure 8. Compared with the ΔI value of CA19-9, the ΔI values of the interferents were much lower, indicating the good specificity of the proposed immunosensor for CA19-9 detection. Moreover, in Figure 7, the reproducibility of the immunosensor was evaluated using the error bars of the different concentrations of CA19-9 of three independent electrodes. The relative standard deviation values of the tests were not more than 1.81% for different CA19-9 concentrations, suggesting the excellent reliability of the fabricated immunosensor.

Application of the immunosensor in human serum samples

The feasibility of the proposed immunosensor for possible clinical application was investigated by analyzing 30 serum samples from The First Affiliated Hospital of Fujian Medical University and People's Liberation Army of China (PLA) 476 hospital. The collection and use of clinical serums obtained from anonymous participants were approved by
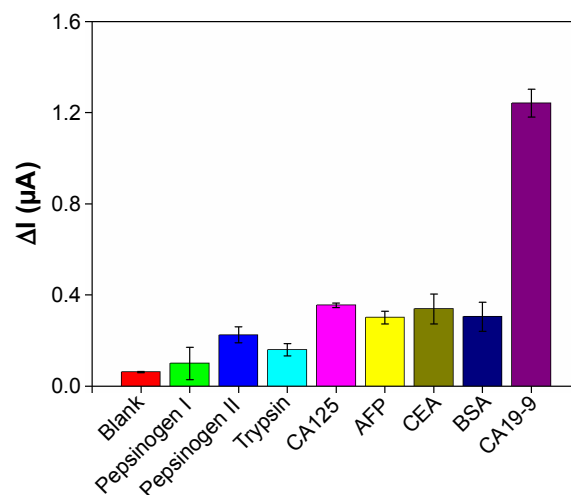
the ethics committee of Fujian Medical University, and the obtained samples were divided into normal control and pancreatic cancer, which was pathologically confirmed. Written informed consent was not obtained from the anonymous participants as this was a retrospective study, and all data was anonymous. Thus, the ethics committee did not require written informed consent from the participants who provided serum sample. According to the ΔI value and the linear equation in Figure 7, the sensing results of the two groups were significantly different and we could qualitatively identify a positive or negative serum specimen, as shown in Figure 9. The positive serum samples of pancreatic cancer showed much higher concentration of CA19-9 than the concentration of CA19-9 of normal control, confirming the clinical
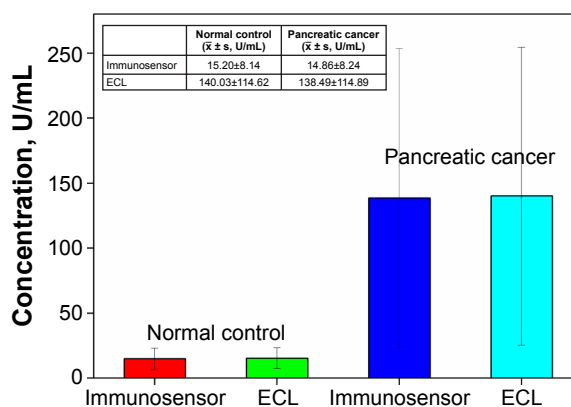

	Normal control (x̄ ± s, U/mL)	Pancreatic cancer (x̄ ± s, U/mL)
Immunosensor	15.20±8.14	14.86±8.24
ECL	140.03±114.62	138.49±114.89

Figure 9 Comparison of detection results between the proposed label-free electrochemical immunosensor and ECL.
Note: Error bars show the varied concentrations of CA19-9 in different clinical samples.
Abbreviations: ECL, electrochemiluminescence; CA19-9, carbohydrate antigen 19-9.

Table 1 Comparison of test results of the proposed label-free electrochemical immunosensor with ECL

Samples	Found by the immunosensor (U/mL)	Found by the ECL (U/mL)	Relative error (%)
Normal control			
1	2.39	2.44	−2.05
2	5.15	5.47	−5.85
3	9.84	9.49	3.69
4	9.25	10	−7.50
5	13	13.95	−6.81
6	17.71	18.59	−4.73
7	18.75	19.58	−4.24
8	20.72	22.48	−7.83
9	25.86	24	7.75
10	25.92	25.99	−0.27
Pancreatic cancer			
11	36.11	39.2	−7.88
12	37.97	40.3	−5.78
13	45.73	48.5	−5.71
14	51.38	56	−8.25
15	65.94	62.3	5.84
16	64.86	63.5	2.14
17	71.55	70.4	1.63
18	81.26	73.5	10.56
19	75.82	76	−0.24
20	83.85	80.3	4.42
21	90.05	88.3	1.98
22	88.26	96.2	−8.25
23	131.3	124.5	5.46
24	144.5	150.8	−4.18
25	189.1	198	−4.49
26	198.9	219	−9.18
27	213.9	227.8	−6.10
28	289.8	276	5.00
29	345.3	360	−4.08
30	464.3	450	3.18

Abbreviation: ECL, electrochemiluminescence.

significance of CA19-9 for the diagnosis and prognostic evaluation of pancreatic cancer.[10] Furthermore, the testing results of the proposed immunosensor and the established electrochemiluminescence (ECL) technique were compared (Table 1). The two methods correlated well with a correlation of 0.998, as shown in Table 2; the P-value of the paired t-test was 0.4 (no significant difference). Moreover, the absolute values of the relative errors of the two methods were lower than 11% (except for one, the others were less than 10%), suggesting the excellent accuracy of the proposed immunosensor for clinical applications. To further elucidate the advantage of the proposed electrochemical immunosensor, the linear range, limit of detection, and clinical applications of the immunosensor were compared with other CA19-9 electrochemical immunosensors. As shown in Table 3, the linear range and limit of detection of the proposed electrochemical immunosensor are comparable, while the proposed method shows the advantage for the detection of the clinical samples due to the reliability, reproducibility, and sensitivity of the fabricated label-free electrochemical immunosensor based on AuNPs@PThi as signal indicator.

Conclusion

In this work, we designed and prepared AuNPs@PThi through a convenient and economical route. The electrochemical response of AuNPs@PThi required the participation of electrons. The immobilization of CA19-9 can cause different electrochemical responses depending on the blocking of the electron transfer before and after immunoreaction. Maximizing the electrochemical properties of AuNPs@

Table 2 Statistics, correlation, and the paired t-test of ELC and the proposed immunosensor

Pair	Serum samples, N	Mean	SD	SEM	Correlation	P-value
ECL	30	98.42	110.50	20.17	0.998	0.4
Immunosensor	30	97.28	110.38	20.15		

Abbreviations: ECL, electrochemiluminescence; SD, standard deviation; SEM, standard error of the mean.

Table 3 Comparison of the sensing performance of different electrochemical immunosensors for CA19-9

Sensing interface	Linear range (U/mL)	Limit of detection (U/mL)	Clinical samples detection	References
Anti-CA19-9/AuNPs/poly(thionine)-SDS nanocomposites	5–400	0.45	Not mentioned	39
Cation-exchange-labeling anti-CA19-9 and methylene blue	5–100	1.6	4 samples	48
Electrochemical microfluidic chip with $K_3[Fe(CN)_6]/K_4[Fe(CN)_6]$	10.75–172	10.75	150 samples	49
HRP-Ab1/TiO$_2$ collosol–gel matrix	3–20	2.68	9 samples	50
ZnO quantum dot-labeled anti-CA19-9	0.1–180	0.04	Not mentioned	51
Anti-CA19-9/3D-ordered macroporous magnetic Au film	0.05–15.65	0.01	4 samples	52
Anti-CA19-9/AuNPs/poly(thionine)-SDS nanocomposites	6.5–520.0	0.26	30 samples containing normal serum and pancreatic cancer serum	This work

Abbreviations: CA19-9, carbohydrate antigen 19-9; HRP, horseradish peroxidase; SDS, sodium dodecyl sulfonate.

PThi, we developed an effective label-free electrochemical immunosensor for the ultrasensitive and reliable detection of CA19-9. The proposed immunosensor showed excellent performance for CA19-9 detection with a remarkable detection limit, acceptable stability, and reproducibility. Furthermore, the proposed assay, which was used to test the clinical serum samples, exhibited accuracy, suggesting the feasibility of the assay in future real applications. In brief, this study suggested an effective strategy for signal amplification based on AuNPs@PThi that can be used to assess CA19-9.

Acknowledgments

Disclosure

The authors report no conflicts of interest in this work.

References

1. Chen WQ, Zheng RS, Baade PD, et al. Cancer statistics in China, 2015. *CA Cancer J Clin*. 2016;66(2):115–132.
2. Audrey V, Joseph H, Rich S, Ralph HH, Michael G. Pancreatic cancer. *Lancet*. 2011;378(9791):607–620.
3. Chari ST. Detecting early pancreatic cancer: problems and prospects. *Semin Oncol*. 2007;34(4):284–294.
4. Chang MC, Wong JM, Chang YT. Screening and early detection of pancreatic cancer in high risk population. *World J Gastroenterol*. 2014; 20(9):2358–2364.
5. Li YX, Sun JJ. MicroRNAs: potential markers for early diagnosis of pancreatic cancer. *Chin J Gen Surg*. 2014;23(5):367–371.
6. Wang Z, Tian YP. Clinical value of serum tumor markers CA19-9, CA125 and CA72-4 in the diagnosis of pancreatic carcinoma. *Mol Clin Oncol*. 2014;2(2):265–268.
7. Huang Z, Liu F. Diagnostic value of serum carbohydrate antigen 19-9 in pancreatic cancer: a meta-analysis. *Tumor Biol*. 2014;35(8): 7459–7465.
8. Duraker N, Hot S, Polat Y, Höbek A, Gençler N, Urhan N. CEA, CA 19-9 and CA 125 in the differential diagnosis of benign and malignant pancreatic diseases with or without jaundice. *J Surg Oncol*. 2007; 95(2):142–147.
9. Imaoka H, Shimizu Y, Senda Y, et al. Post-adjuvant chemotherapy CA19-9 levels predict prognosis in patients with pancreatic ductal adenocarcinoma: a retrospective cohort study. *Pancreatology*. 2016; 16(4):658–664.
10. Humphris JL, Chang DK, Johns AL, et al; NSW Pancreatic Cancer Network. The prognostic and predictive value of serum CA19.9 in pancreatic cancer. *Ann Oncol*. 2012;23(7):1713–1722.
11. Tian JN, Zhou LJ, Zhao YC, Wang Y, Peng Y, Zhao SL. Multiplexed detection of tumor markers with multicolor quantum dots based on fluorescence polarization immunoassay. *Talanta*. 2012;92(1):72–77.
12. Chang YF, Yu JS, Chang YT, et al. The utility of a high-throughput scanning biosensor in the detection of the pancreatic cancer marker ULBP2. *Biosens Bioelectron*. 2013;41(6):232–237.
13. Hwang H, Chon H, Choo J, Park JK. Optoelectrofluidic sandwich immunoassays for detection of human tumor marker using surface-enhanced Raman scattering. *Anal Chem*. 2010;82(18):7603–7610.
14. Hu SH, Zhang SC, Hu ZC, Xing Z, Zhang XR. Detection of multiple proteins on one spot by laser ablation inductively coupled plasma mass spectrometry and application to immuno-micmarray with element-tagged antibodies. *Anal Chem*. 2007;79(3):923–929.
15. Yu XM. The clinical application of chemiluminescence enzyme immunoassay for primary hepatocellular carcinoma tumor markers. *J Community Med*. 2015;13(14):1–2.
16. Chen Z, Wu J, Chen W, Huang XJ, Yan F. Chemiluminescence imaging immunoassay of multiple tumor markers for cancer screening. *Anal Chem*. 2012;84(5):2410–2415.
17. Lintermans A, Asten KV, Wildiers H, et al. Abstract P1-13-08: arthralgia and changes in serum levels of IGF-I, its binding protein and estrogen in breast cancer patients on endocrine agents. *Cancer Res*. 2013; 73(24 suppl):P1-13-08.
18. Yan L, Li Z, Zhang Y. Aflatoxins in milk by radio immunoassay method. *Food Res Dev*. 2010;31(1):135–137.
19. Jiang J, Zhao SL, Huang Y, Qin GX, Ye FG. Highly sensitive immunoassay of carcinoembryonic antigen by capillary electrophoresis with gold nanoparticles amplified chemiluminescence detection. *J Chromatogr A*. 2013;1282(5):161–166.
20. Mehta PK, Raj A, Singh NP, Khuller GK. Detection of potential microbial antigens by immuno-PCR (PCR-amplified immunoassay). *J Med Microbiol*. 2014;63(5):627–641.
21. Robinson KJ, Hazon N, Lonergan M, Pomeroy PP. Validation of an enzyme-linked immunoassay (ELISA) for plasma oxytocin in a novel mammal species reveals potential errors induced by sampling procedure. *J Neurosci Methods*. 2014;226(8):73–79.
22. Halbmayr-Jech E, Hammer E, Fielder R, Coutts J, Rogers A, Cornish M. Characterization of G12 sandwich ELISA, a next-generation immunoassay for gluten toxicity. *J AOAC Int*. 2012;95(2):372–376.
23. Manuel PC, Antonio CC, Elisabet CP, et al. Discovery and validation of an INflammatory PROtein-driven GAstric cancer Signature (INPRO-GAS) using antibody microarray-based oncoproteomics. *Oncotarget*. 2014;5(7):1942–1954.
24. Luo L, Dong LY, Yan QG, et al. Research progress in applying proteomics technology to explore early diagnosis biomarkers of breast cancer, lung cancer and ovarian cancer. *Asian Pac J Cancer Prev*. 2014; 15(20):8529–8538.
25. Schmitz-Dräger BJ, Droller M, Lokeshwar VB, et al. Molecular markers for bladder cancer screening, early diagnosis, and surveillance: The WHO/ICUD Consensus. *Urol Int*. 2015;94(1):1–24.
26. Crespo GA, Mistlberger G, Bakker E. Electrogenerated chemiluminescence for potentiometric sensors. *J Am Chem Soc*. 2012;134(1):205–207.
27. Wei YC, Li Y, Li N, et al. Sandwich-type electrochemical immunosensor for the detection of AFP based on Pd octahedral and APTES-M-CeO$_2$-GS as signal labels. *Biosens Bioelectron*. 2016;79:482–487.
28. Brondani D, Piovesan JV, Westphal E, et al. A label-free electrochemical immunosensor based on an ionic organic molecule and chitosan-stabilized gold nanoparticles for the detection of cardiac troponin T. *Analyst*. 2014;139(20):5200–5208.
29. Santharamana P, Dasb M, Singhc SK, et al. Label-free electrochemical immunosensor for the rapid and sensitive detection of the oxidative stress marker superoxide dismutase 1 at the point-of-care. *Sens Actuat B Chem*. 2016;236:546–553.

30. Wang YL, Li YY, Ma HM, et al. Label-free electrochemical immunosensor with novel signal production and amplification strategy based on three-dimensional pine-like Au-Cu nanodendrites. *RSC Adv*. 2015; 5(40):31262–31269.

31. Carneiro P, Loureiro J, Delerue-Matos C, Morais S, Pereira MDC. Alzheimer's disease: development of a sensitive label-free electrochemical immunosensor for detection of amyloid beta peptide. *Sens Actuat B Chem*. 2016;239:157–165.

32. Bromfield SM, Barnard A, Posocco P, Fermeglia M, Pricl S, Smith DK. Mallard blue: a high-affinity selective heparin sensor that operates in highly competitive media. *J Am Chem Soc*. 2013;135(2):2911–2913.

33. Huo KF, Gao B, Fu JJ, Zhao LZ, Chu PK. Fabrication, modification, and biomedical applications of anodized TiO$_2$ nanotube arrays. *RSC Adv*. 2014;4(33):17300–17324.

34. Liu XF, Ouyang L, Cai XH, et al. An ultrasensitive label-free biosensor for assaying of sequence-specific DNA-binding protein based on amplifying fluorescent conjugated polymer. *Biosens Bioelectron*. 2013; 41(15):218–224.

35. Kang D, Ricci F, White RJ, Plaxco KW. Survey of redox-active moieties for application in multiplexed electrochemical biosensors. *Anal Chem*. 2016;88(21):10452–10458.

36. Wang H, Ohnuki H, Endo H, Izumi M. Impedimetric and amperometric bifunctional glucose biosensor based on hybrid organic-inorganic thin films. *Bioelectrochemistry*. 2015;101:1–7.

37. Han JM, Ma J, Ma ZF. One-step synthesis of graphene oxide–thionine–Au nanocomposites and its application for electrochemical immunosensing. *Biosens Bioelectron*. 2013;47(10):243–247.

38. Dai YL, Li XY, Fan LM, Lu XJ, Kan XW. "Sign-on/off" sensing interface design and fabrication for propyl gallate recognition and sensitive detection. *Biosens Bioelectron*. 2016;86:741–747.

39. Jiang ZQ, Zhao CF, Lin LQ, Weng SH, Liu QC, Lin XH. A label-free electrochemical immunosensor based on poly(thionine)-SDS nanocomposites for CA19-9 detection. *Anal Methods*. 2015;7(11):4508–4513.

40. Weng SH, Liu QC, Zhao CF, et al. Sensitive electrochemical immunoassay based on polythionine-Au nanocomposites as enhanced sensing signal for selective detection of biomarker with high isoelectric point. *Sens Actuat B Chem*. 2015;216:307–315.

41. Cai XH, Weng SH, Guo RB, et al. Ratiometric electrochemical immunoassay based on internal reference value for reproducible and sensitive detection of tumor marker. *Biosens Bioelectron*. 2016;81: 173–180.

42. Zhao CF, Jiang ZJ, Cai XH, Lin LQ, Lin XH, Weng SH. Ultrasensitive and reliable dopamine sensor based on polythionine/AuNPs composites. *J Electroanal Chem*. 2015;748:16–22.

43. Ou CF, Yuan R, Chai YQ, Tang MY, Chai R, He XL. A novel amperometric immunosensor based on layer-by-layer assembly of gold nanoparticles-multi-walled carbon nanotubes-thionine multilayer films on polyelectrolyte surface. *Anal Chim Acta*. 2007;603(2):205–213.

44. Shi WT, Ma ZF. A novel label-free amperometric immunosensor for carcinoembryonic antigen based on redox membrane. *Biosens Bioelectron*. 2011;26(6):3068–3071.

45. Weng SH, Chen M, Zhao CF, et al. Label-free electrochemical immunosensor based on K3[Fe(CN)6] as signal for facile and ultrasensitive determination of tumor necrosis factor-alpha. *Sens Actuat B Chem*. 2013;184:1–7.

46. Chen M, Zhao CF, Chen W, et al. Sensitive electrochemical immunoassay of metallothionein-3 based on K3[Fe(CN)6] as a redox-active signal and C-dots/Nafion film for antibody immobilization. *Analyst*. 2013;138(24):7341–7346.

47. Liu N, Chen X, Ma ZF. Ionic liquid functionalized graphene/Au nanocomposites and its application for electrochemical immunosensor. *Biosens Bioelectron*. 2013;48:33–38.

48. Wang GJ, Qing Y, Shan JL, Jin F, Yuan R, Wang D. Cation-exchange antibody labeling for simultaneous electrochemical detection of tumor markers CA15-3 and CA19-9. *Microchimica Acta*. 2013;180(7–8): 651–657.

49. Xie Y, Zhi X, Su HC, et al. A novel electrochemical microfluidic chip combined with multiple biomarkers for early diagnosis of gastric cancer. *Nanoscale Res Lett*. 2015;10(1):1–9.

50. Du D, Yan F, Liu SL, Ju HX. Immunological assay for carbohydrate antigen 19-9 using an electrochemical immunosensor and antigen immobilization in titania sol–gel matrix. *J Immunol Methods*. 2003; 283(1–2):67–75.

51. Gu BX, Xu GX, Yang C, Liu SQ, Wang ML. ZnO quantum dot labeled immunosensor for carbohydrate antigen 19-9. *Biosens Bioelectron*. 2011;26(5):2720–2723.

52. Zhang Q, Chen XJ, Tang Y, Ge LN, Guo BH, Yao C. Amperometric carbohydrate antigen 19-9 immunosensor based on three dimensional ordered macroporous magnetic Au film coupling direct electrochemistry of horseradish peroxidase. *Anal Chim Acta*. 2014;815(815):42–50.